

Self-Assembly of Amphoteric Azopyridine Carboxylic Acids: Organized Structures and Macroscopic Organized Morphology Influenced by Heat, pH Change, and Light

Ken'ichi Aoki, Masaru Nakagawa, and Kunihiro Ichimura*

Contribution from the Chemical Resources Laboratory, Tokyo Institute of Technology, 4259 Nagatsuta, Midori-ku, Yokohama 226-8503, Japan

Received May 22, 2000

Abstract: In this paper, we describe the synthesis of novel amphoteric azopyridine carboxylic acids (**2b**, **3a**, **3b**, **4a**, and **4b**), having both a carboxyl group as a hydrogen donor and a pyridyl group as an acceptor at each molecular terminus, and their self-organization, which is markedly affected by external stimuli including heat, pH changes, and light. The amphoteric compounds form intermolecular hydrogen bonds between pyridyl and carboxyl groups in a head-to-tail manner in the solid state to give linear pseudopolymer structures, as supported by FT-IR analysis. Heating and cooling across their melting points induced thermoreversible supramolecular depolymerization to and polymerization from small molecular components of monomers and the corresponding carboxylic acid dimers. In alkaline aqueous media, these amphoteric compounds, dissolved as carboxylate anions, were gradually neutralized by atmospheric carbon dioxide, leading to their deposition as novel fibrous materials from **3b** and **4b**, substituted with a propyl group at the phenyl ring, and as leaflet crystals from **3a** and **4a** bearing no substituent. FT-IR and X-ray diffraction measurements supported the conclusion that the formation of fibrous materials from **3b** and **4b** arises from their intermolecular hydrogen bonding in a head-to-tail manner as well as the suppressive effect of propyl substitution on the π - π stacking of the molecules. UV irradiation of alkaline solutions of **4b** resulted in the modification of the morphology of fibrous materials, probably because the photoisomerized Z-isomer of **4b** affected the nucleation process in the fibrous formation. These results suggest that morphological properties of these macroscopic self-assemblages are tunable by appropriate choices of environmental stimuli such as heat, pH, and light.

Introduction

The levels of noncovalent intermolecular interactions such as hydrogen bondings, π - π stackings, metal-ligand interactions, charge-transfer interactions, and so on, which are employed and designed to assemble supramolecular architectures, are determined to a significant extent not only by the chemical structures of the component molecules, but also by environmental factors, including the properties of the media in which the starting molecules are dissolved. As seen in biological systems such as deoxyribonucleic acids, optimizing such noncovalent molecular interactions by environmental factors has the most significant effect in the creation of intricate supramolecular assemblages and the emergence of highly sophisticated functionalities.¹ Such noncovalent intermolecular interactions have been extensively utilized in the field of supramolecular chemistry to construct many kinds of supramolecules, such as complexes of crown ethers, cryptands, and so forth with selective alkali metal cations.² Further advances in supramolecular chemistry have allowed the formation of assorted three-dimensional architectures, which may enable us to create fine

nano- or microscale structures. Kunitake et al. studied previously the self-organization of various kinds of synthetic single- and double-chain ammonium amphiphiles to discuss the relationship between aggregate morphology and chemical structure of the amphiphiles in aqueous media.³ Several kinds of structural components, including hydrocarbon flexible tails and spacers, mesogenic rigid segments, and hydrophilic headgroups, determine the aggregates morphology of amphiphiles and their stability.^{3e} Later, Fuhrhop et al. reported for the first time the formation of stable fibrous assemblages made from amphiphiles with an aldonamide headgroup,⁴ demonstrating that the intermolecular hydrogen bonding of secondary amide groups markedly stabilizes the molecular assemblages.⁵ That work was followed more recently by reports on the analogous solidlike

* To whom correspondence should be addressed. Telephone: +81-45-924-5266. Fax: +81-45-924-5276. E-mail: kichimur@res.titech.ac.jp.

(1) (a) Jeffrey, G. A. *An Introduction to Hydrogen Bonding*; Oxford University Press: New York, 1997; pp 184–212. (b) Jeffrey, G. A.; Saenger, W. *Hydrogen bonding in biological structures*; Springer-Verlag: Berlin, 1991; pp 309–422.

(2) (a) Lehn, J. M. *Supramolecular Chemistry*; VCH: Weinheim, 1995; pp 11–30. (b) Lehn, J. M. *Science* **1985**, 227, 849. (c) Lehn, J. M. *Angew. Chem., Int. Ed. Engl.* **1988**, 27, 89.

(3) (a) Okahata, Y.; Kunitake, T. *J. Am. Chem. Soc.* **1979**, 101, 5231. (b) Kunitake, T.; Okahata, Y. *J. Am. Chem. Soc.* **1980**, 102, 549. (c) Kunitake, T.; Nakashima, N.; Morimitsu, K. *Chem. Lett.* **1980**, 1347. (d) Kunitake, T.; Nakashima, N.; Simomura, M.; Okahata, Y. *J. Am. Chem. Soc.* **1980**, 102, 6642. (e) Kunitake, T.; Okahata, Y.; Simomura, M.; Yasunami, S.; Takarabe, K. *J. Am. Chem. Soc.* **1981**, 103, 5401. (f) Nakashima, N.; Fukushima, H.; Kunitake, T. *Chem. Lett.* **1981**, 1207. (g) Nakashima, N.; Asakuma, S.; Kim, J.-M.; Kunitake, T. *Chem. Lett.* **1984**, 1709. (h) Nakashima, N.; Asakuma, S.; Kunitake, T. *J. Am. Chem. Soc.* **1985**, 107, 509. (i) Kunitake, T.; Yamada, N. *J. Chem. Soc., Chem. Commun.* **1986**, 655.

(4) (a) Fuhrhop, J.-H.; Schnieder, P.; Rosenberg, J.; Boekema, E. *J. Am. Chem. Soc.* **1987**, 109, 3387. (b) Fuhrhop, J.-H.; Schnieder, P.; Boekema, E.; Helfrich, W. *J. Am. Chem. Soc.* **1988**, 110, 2861. (c) Fuhrhop, J.-H.; Boettcher, C. *J. Am. Chem. Soc.* **1990**, 112, 1768. (d) Fuhrhop, J.-H.; Svenson, S.; Boettcher, C.; Rössler, E.; Vieth, H.-M. *J. Am. Chem. Soc.* **1990**, 112, 4307.

(5) Fuhrhop, J. H.; Helfrich, W. *Chem. Rev.* **1993**, 93, 1565.

fibrous materials formed from other amphiphiles of phospholipid derivatives,⁶ glucosamide bolaamphiphiles,⁷ amino acid derivatives,⁸ and others.⁹ Moreover, Shimizu et al. reported on precisely controlled microtubes encapsulating a number of vesicular assemblages inside their aqueous compartment, using bolaamphiphiles with carboxylic headgroups at both molecular ends.¹⁰ These molecular assemblages are ultimately associated with natural biological systems.

For the construction of the well-defined molecular assemblages mentioned above, hydrogen bonds are regarded as an essential driving force because their moderate and reversible nature differs intrinsically from that of covalent bonds. Such characteristics of hydrogen bonding give rise to specific functionalities of artificial materials as well as biological materials. Kato et al.¹¹ and Griffin et al.¹² reported on hydrogen-bonded supramolecular liquid crystals and liquid crystalline polymers with the goal of their application to optical elements. In the other cases, the formation of hydrogen-bonded fibrous nanoscale networks gave rise to the gelation of a variety of solvents.¹³ Without such hydrogen bonding, anthracene derivatives,¹⁴ steroid derivatives,¹⁵ and steroidal and condensed aromatic rings¹⁶ form gels with various kinds of organic solvents,¹⁷ suggesting that intermolecular interactions involving

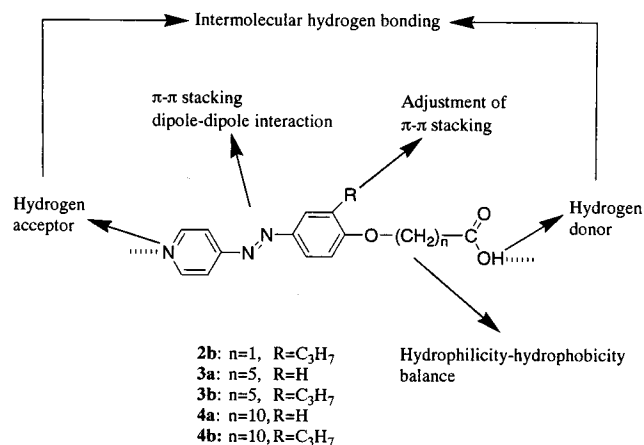


Figure 1. Azopyridine carboxylic acids (**2b**, **3a**, **3b**, **4a**, and **4b**).

van der Waals interactions among aromatic rings or hydrophobic cyclic hydrocarbons also play an important role in molecular assembly.

Knowing that the self-organization of molecular assemblages possessing highly ordered structures is decisively governed by the chemical structures of the original low-molecular-weight molecules, we anticipate that the macroscopic morphological shapes of the molecular assemblages should be modulated by the modification of original molecules by external physical or chemical stimuli such as light, heat, and pH changes. This is because molecular-level alteration by external stimuli should be amplified in molecular assemblages at the macroscopic level during the self-organization process through multiple intermolecular interactions.¹⁸ Indeed, several studies have shown that morphological features of organic tubes (length distribution and thickness of wall) and of low-molecular-weight gels can be controlled by varying the preparation conditions such as concentrations of lipids, solvents, cooling rates, and light.^{16c,19} Our investigation has been concentrated on the control of the macroscopic morphology of self-organized materials by external physical stimuli such as light.

We started by designing simple organic molecules to give molecular assemblages which might lead to a better understanding of the relationships between monomolecular chemical structure and macroscopic morphological features. Kato et al. demonstrated that novel supramolecular liquid crystals are formed through a pyridyl/carboxyl hydrogen bond when two kinds of organic molecules possessing either a pyridyl group as a hydrogen acceptor or a carboxyl group as a hydrogen donor are mixed.¹¹ Griffin et al. reported that binary mixtures of bola-form organic compounds bearing either two carboxyl groups or pyridyl groups at both molecular termini give rise to supramolecular polymerization through formation of hydrogen bonds between their carboxyl and pyridyl groups, and that the resulting hydrogen-bonded materials exhibit rheological properties similar to those of conventional linear polymers formed through covalent bonds.¹² Taking these facts into consideration, we designed a novel family of amphoteric azopyridine carboxylic acids possessing both a carboxyl group as a hydrogen donor and a pyridyl group as a hydrogen acceptor at each molecular terminus, as shown in Figure 1 on the basis of the

(17) Terech, P.; Weiss, R. G. *Chem. Rev.* **1997**, *97*, 3133. References to the other gelators are given therein.

(18) Ichimura, K. *Chem. Rev.* **2000**, *100*, 1847.

(19) (a) Thomas, B. N.; Safinya, C. R.; Plano, R. J.; Clark, N. A. *Science* **1995**, *267*, 1635. (b) Spector, M. S.; Selinger, J. V.; Singh, A.; Rodrigues, J. M.; Price, R. R.; Schnur, J. M. *Langmuir* **1998**, *14*, 3493. (c) Spector, M. S.; Price, R. R.; Schnur, J. M. *Adv. Mater.* **1999**, *11*, 337.

(6) (a) Yanagawa, H.; Ogawa, Y.; Furuta, H.; Tsuno, K. *J. Am. Chem. Soc.* **1989**, *111*, 4567. (b) Takeoka, S.; Sakai, H.; Iwai, H.; Ohono, H.; Tsuchida, E. *Polym. Prepr., Jpn.* **1989**, *38*, 568.

(7) (a) Shimizu, T.; Masuda, M. *J. Am. Chem. Soc.* **1997**, *119*, 2812. (b) Kogiso, M.; Hanada, T.; Yase, K.; Shimizu, T. *Chem. Commun.* **1998**, 1791. (c) Masuda, M.; Hanada, T.; Yase, K.; Shimizu, T. *Macromolecules* **1998**, *31*, 9403. (d) Nakazawa, I.; Masuda, M.; Okada, Y.; Hanada, T.; Yase, K.; Asai, M.; Shimizu, T. *Langmuir* **1999**, *15*, 4757.

(8) Imae, T.; Takahashi, Y.; Muramatsu, H. *J. Am. Chem. Soc.* **1992**, *114*, 3414.

(9) (a) Menger, F. M.; Lee, S. J. *J. Am. Chem. Soc.* **1994**, *116*, 5987. (b) Imae, T.; Ikeda, Y.; Iida, M.; Koine, N.; Kaizaki, S. *Langmuir* **1998**, *14*, 5631.

(10) (a) Shimizu, T.; Kogiso, M.; Masuda, M. *Nature* **1996**, *383*, 487. (b) Kogiso, M.; Ohnishi, S.; Yase, K.; Masuda, M.; Shimizu, T. *Langmuir* **1998**, *14*, 4978.

(11) (a) Kato, T.; Fréchet, J. M. J. *J. Am. Chem. Soc.* **1989**, *111*, 8533. (b) Kato, T.; Fréchet, J. M. J.; Wilson, P. G.; Saito, T.; Uryu, T.; Fujishima, A.; Jin, C.; Kaneuchi, F. *Chem. Mater.* **1993**, *5*, 1094. (c) Kato, T.; Fréchet, J. M. J., *Macromol. Symp.* **1995**, *98*, 311. (d) Kihara, H.; Kato, T.; Uryu, T.; Fréchet, J. M. J. *Chem. Mater.* **1996**, *8*, 961. (e) Kato, T. *Struct. Bonding* **2000**, *96*, 95.

(12) (a) Alexander, C.; Jariwala, C. P.; Lee, C.-M.; Griffin, A. C. *Macromol. Symp.* **1994**, *77*, 283. (b) Lee, C.-M.; Jariwala, C. P.; Griffin, A. C. *Polymer* **1994**, *35*, 4550. (c) Lee, C.-M.; Griffin, A. C. *Macromol. Symp.* **1997**, *117*, 281.

(13) (a) Tachibana, T.; Kitazawa, S.; Takeno, H. *Bull. Chem. Soc. Jpn.* **1970**, *43*, 2418. (b) Terech, P.; Rodriguez, V.; Barnes, J. D.; McKenna, B. *Langmuir* **1994**, *10*, 3406. (c) Amanokura, N.; Yoza, K.; Shinmori, H.; Shinkai, S.; Reinhoudt, D. N. *J. Chem. Soc., Perkin Trans. 2* **1998**, 2585. (d) Aoki, M.; Nakashima, K.; Kawabata, H.; Tsutsui, S.; Shinkai, S. *J. Chem. Soc., Perkin Trans. 2* **1993**, 347. (e) Hanabusa, K.; Hiratsuka, K.; Kimura, M.; Shirai, H. *Chem. Mater.* **1999**, *11*, 649. (f) Hanabusa, K.; Okui, K.; Karaki, K.; Kimura, M.; Shirai, H. *J. Colloid Interface Sci.* **1997**, *195*, 86. (g) Hanabusa, K.; Matsumoto, Y.; Miki, T.; Koyama, T.; Shirai, H. *J. Chem. Soc., Chem. Commun.* **1994**, 1401. (h) Schoonbeek, F. S.; van Esch, J. H.; Wegewijs, B.; Rep, D. B. A.; de Haas, M. P.; Klapwijk, T. M.; Kellogg, R. M.; Feringa, B. L. *Angew. Chem., Int. Ed.* **1999**, *38*, 1393. (i) Terech, P.; Allegraud, J. J.; Garner, C. M. *Langmuir* **1998**, *14*, 3991.

(14) (a) Clavier, G. M.; Brugger, J.-F.; Bouas-Laurent, H.; Pozzo, J.-L. *J. Chem. Soc., Perkin Trans. 2* **1998**, 2527. (b) Pozzo, J.-L.; Clavier, G. M.; Colomes, M.; Bouas-Laurent, H. *Tetrahedron* **1997**, *53*, 6377. (c) Terech, P.; Bouas-Laurent, H.; Desvergne, J. P. *J. Colloid Interface Sci.* **1995**, *174*, 258. (d) Desvergne, J.-P.; Fages, F.; Bouas-Laurent, H.; Marsau, P. *Pure Appl. Chem.* **1992**, *64*, 1231.

(15) (a) Bujanowsky, V. J.; Katsoulis, D. E.; Ziemelis, M. *J. Mater. Chem.* **1994**, *4*, 1181. (b) Terech, P.; Berthet, C. *J. Phys. Chem.* **1988**, *92*, 4269. (c) Terech, P. *J. Colloid Interface Sci.* **1985**, *107*, 244. (d) Terech, P. *Mol. Cryst. Liq. Cryst.* **1989**, *166*, 29.

(16) (a) Mukkamala, R.; Weiss, R. G. *Langmuir* **1996**, *12*, 1474. (b) Terech, P.; Ostuni, E.; Weiss, R. G. *J. Phys. Chem.* **1996**, *100*, 3759. (c) Geiger, C.; Stanesco, M.; Chen, L.; Whitten, D. G. *Langmuir* **1999**, *15*, 2241.

following. First, the amphoteric compounds should form pseudolinear polymers, based on intermolecular hydrogen bonds forming between the pyridyl and carboxyl groups in a head-to-tail manner. Second, a dipole moment arising intrinsically from the asymmetrical molecular structure of the amphoteric molecules should enhance dipole–dipole interactions among the molecules, leading to their molecular stacking, extending the information that may be obtained about the monomolecular chemical structure to three-dimensional macroscopic molecular aggregates. Third, it is likely that the occurrence of intermolecular hydrogen bonds in a head-to-tail manner is significantly dependent on the pH value of the medium because the amphoteric compounds have an ionizable carboxyl group. Fourth, since aromatic azo compounds undergo *E/Z* photoisomerization,²⁰ it is anticipated that the photoinduced alteration of their molecular geometry causes the transformation of macroscopic molecular assemblages. Consequently, the amphoteric azopyridine carboxylic acids should respond to a variety of external stimuli such as light, pH change of the medium, and heat, leading to the on-demand control of macroscopic molecular assemblages. In addition, these compounds offer advantages in the simplicity of their monomolecular chemical structure when compared with those in a majority of the previous reports. This fact should serve to deepen the understanding of the relationship between the monomolecular chemical structure and the morphology of organized materials. We report first the formation of novel fibrous materials starting from two azopyridine carboxylic acids, which are substituted with a propyl group at one of the aromatic rings, followed by the structural analysis of molecular assemblages to reveal the contribution of the propyl side-chain substituent. Subsequently, the possibility to control the formation of molecular assemblages by controlling external stimuli including heat application, pH changes, and light irradiation is discussed.

During our extensive studies on amphoteric compounds of this kind since our first report,²¹ closely related work has been recently reported on the thin-film organization of linear polymeric assemblages formed from a one-component molecule in a head-to-tail hydrogen-bonded manner, which is fabricated by organic molecular beam deposition methods.²² The major purpose of these papers is to reveal second harmonic generation arising from the asymmetrical character of the organized thin-film materials.

Results

Synthesis and Thermal Properties of Azopyridine Carboxylic Acids. Amphoteric azopyridine carboxylic acids were synthesized in three steps, involving the azo coupling of a phenol with 4-aminopyridine, the Williamson ether synthesis with ω -bromoalkanoate, and subsequent alkaline hydrolysis. The azopyridine carboxylic acids without a side-chain substituent (**3a** and **4a**) showed little solubility in organic solvents except

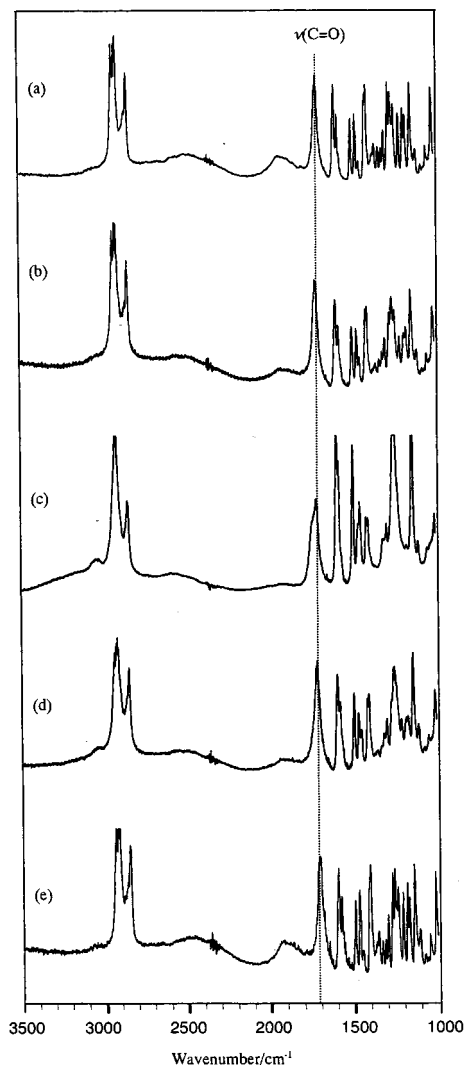


Figure 2. FT-IR spectra of **4a** at (a) 50, (b) 170, and (c) 180 °C on heating and at (d) 170 and (e) 50 °C on cooling.

for acidic or basic solvents such as acetic acid and pyridine, while the other derivatives, with a propyl substituent on an aromatic ring of the azopyridine moiety (**2b**, **3b**, and **4b**), exhibited improved solubility in common organic solvents such as tetrahydrofuran, acetone, and chloroform. The thermal properties of each compound were investigated by means of DSC analysis. As observed for **3b** and **4b** (mp 172 °C for **3b** and 152 °C for **4b**), the introduction of a propyl substituent to **3a** and **4a** led to a significant lowering of their melting points (229 °C for **3a** and 173 °C for **4a**), presumably due to the alteration of intermolecular interactions involving π – π stacking, dipole–dipole interactions, and hydrogen bonding arising from the side-chain substituent effect.

Temperature-dependent FT-IR spectra provide valuable information concerning thermally induced changes in the assembled molecular structures of hydrogen-bonded materials.¹¹ As shown in Figure 2a, the FT-IR spectrum of **4a** at 50 °C exhibits $\nu_{C=O}$, ν_{OH} , and its Fermi resonance bands at 1707, 2500, and 1930 cm^{-1} , respectively. The same infrared spectral features have been reported for several hydrogen-bonded complexes formed from a binary mixture of pyridine and carboxylic acid derivatives.²³ Therefore, these characteristic bands are ascribed to the formation of consecutive intermolecular hydrogen bonds in a head-to-tail manner between the

(20) (a) Crano, J. C.; Guglielmetti, R. J. *Organic Photochromic and Thermochromic Compounds, Volume 2*; Kluwer Academic/Plenum Publishers: New York, 1999; pp 9–63. (b) Dürr, H.; Bouas-Laurent, H. *Photochromism, Molecules and Systems*; Elsevier: Amsterdam, 1990; pp 165–192.

(21) (a) Aoki, K.; Nakagawa, M.; Morino, S.; Seki, T.; Ichimura, K. *Prepr. Chem. Soc. Jpn.* **1998**, 1390. (b) Aoki, K.; Nakagawa, M.; Ichimura, K. *Chem. Lett.* **1999**, 1205.

(22) (a) Cai, C.; Bösch, M. M.; Tao, Y.; Müller, B.; Kündig, A.; Bosshard, C.; Günter, P. *Polym. Prepr. (Am. Chem. Soc., Div. Polym. Chem.)* **1998**, 39, 1069. (b) Cai, C.; Bösch, M. M.; Tao, Y.; Müller, B.; Gan, Z.; Bosshard, C.; Liakatas, I.; Jäger, M.; Günter, P. *J. Am. Chem. Soc.* **1998**, 120, 8563. (c) Cai, C.; Müller, B.; Weckesser, J.; Barth, J. V.; Tao, Y.; Bösch, M. M.; Kündig, A.; Bosshard, C.; Biaggio, I.; Günter, P. *Adv. Mater.* **1999**, 11, 750. (d) Müller, B.; Cai, C.; Kündig, A.; Tao, Y.; Bösch, M.; Jäger, M.; Bosshard, C.; Günter, P. *Appl. Phys. Lett.* **1999**, 74, 3110.

(23) Johnson, S. L.; Rumon, K. A. *J. Phys. Chem.* **1965**, 69, 74.

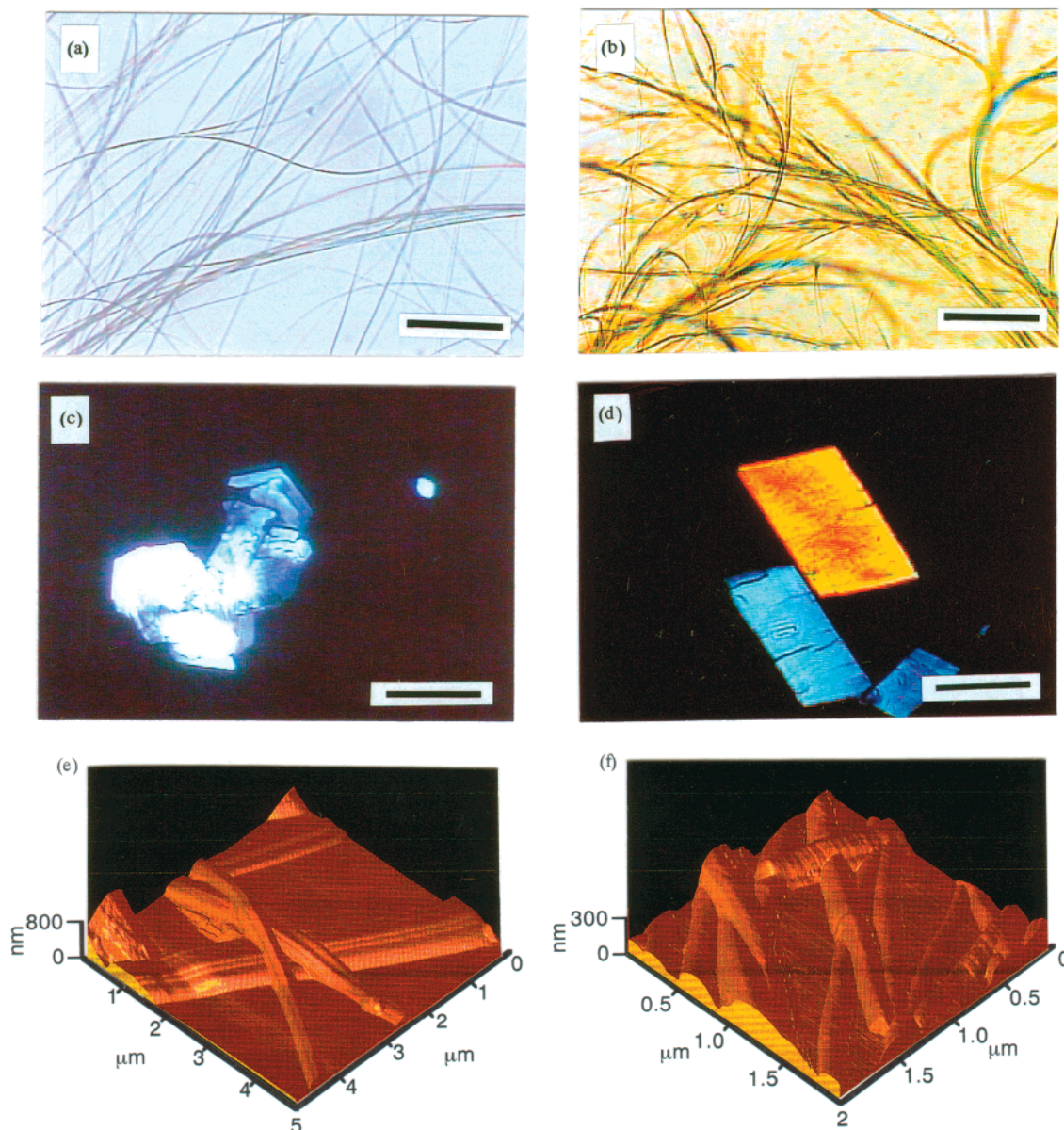


Figure 3. Optical microscopy images of fibrous materials formed from (a) **3b** and (b) **4b**; polarized optical microscopy images of leaflet crystals formed from (c) **3a** and (d) **4a** (scale bar: 10 μm); and AFM images of microfibers formed from (e) **3b** (5 \times 5 μm) and (f) **4b** (2 \times 2 μm).

pyridyl and carboxyl groups of **4a** in the solid state, leading to the self-organization of a pseudopolymer structure by a single-component molecule, as depicted in Figure 1. Similar spectral features were also observed for the other amphoteric azopyridine carboxylic acids of **3a**, **3b**, and **4b** in the solid state. No significant spectral change was observed in Figure 2b upon heating from 50 to 170 $^{\circ}\text{C}$, while further heating to 180 $^{\circ}\text{C}$, beyond the melting point of **4a** (at 173 $^{\circ}\text{C}$), caused abrupt spectral changes involving the disappearance of ν_{OH} and its Fermi resonance bands and the shift of the $\nu_{\text{C=O}}$ band to a higher wavenumber (Figure 2c). The spectral changes were accompanied by the appearance of a broad band around 3000 cm^{-1} , assignable to a ν_{OH} band derived from the formation of the carboxylic acid dimer of **4a**. These spectral changes were completely reversible upon heating and cooling across the melting point, suggesting that the pseudopolymer chains formed through hydrogen bonding between the pyridyl and carboxyl groups in a head-to-tail manner undergo thermoreversible polymerization from and depolymerization to small component molecules such as monomeric **4a** and/or its dimers.

Self-Organization in Aqueous Media. A. Self-Organization Behavior. When a 1 mmol dm^{-3} aqueous solution of either **3b** or **4b** containing a 10 molar equivalent amount of NaOH was left to stand for several days under atmospheric conditions, self-organization into well-defined microfibers occurred. Parts a and b of Figure 3 show optical microscopy images of typical microfibers made from **3b** and **4b**, respectively. The microfibers are more than several hundred micrometers in length and 1 μm in diameter. The microfibers of **3b** and **4b** were formed at about pH 9 and 10, respectively, and their morphology was highly stable in the aqueous medium for several months. Both of the yield and the shape of the microfibers were independent of the initial concentration of **4b** in the range of 2×10^{-5} – 10^{-2} mol dm^{-3} . AFM images of dried fibers, shown in Figure 4e,f, indicate that the microfibers of **3b** and **4b** are composed of bundles of submicrofibers with an almost uniform diameter of 350 and 200 nm, respectively. In contrast to **3b** and **4b**, azopyridine carboxylic acid, with a shorter spacer length (**2b**), failed to self-organize into fibrous assemblages. The azopyridine carboxylic acid without the propyl substituent (**3a**) formed

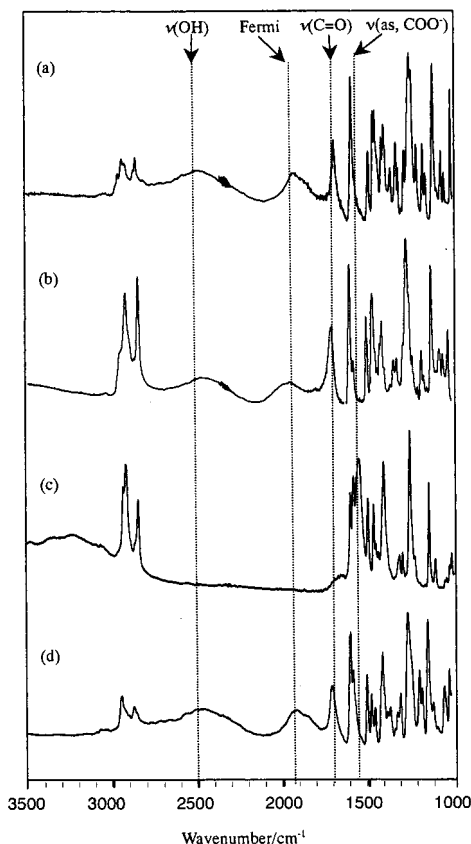


Figure 4. FT-IR spectra of the molecular assemblages formed from (a) **3a**, (b) **3b**, (c) **4a**, and (d) **4b**.

crystalline leaflets under the same conditions, as shown in Figure 3c. **4a** gave also leaflet crystals (Figure 3d) from the alkaline solution of the mixture of water and THF (3:1 v/v). The influence of THF on the formation of the microfibers of **4b** was ignored since microfibers with an analogous morphological feature were deposited from the mixed solvent of water and THF. Taking the difference in morphological features between **3a** and **3b** or **4a** and **4b** into consideration, we can conclude that the propyl side-chain substituent on the azopyridine moiety is necessary in order for the microfibers to be formed.

B. Elemental Analysis. The elemental analysis of fibers dried in vacuo gave a chemical composition of C, 67.24%; H, 6.82%; N, 11.75% for **3b** and C, 70.12%; H, 8.28%; N, 9.97% for **4b**. These results are consistent with those for pure samples of **3b** (C, 67.58%; H, 7.09%; N, 11.82%) and **4b** (C, 70.56%; H, 8.29%; N, 9.87%), revealing that the fibrous materials are hardly contaminated by sodium ion, even when formed in alkaline aqueous solutions. The elemental analysis of leaflet crystals of **3a** and **4a** exhibited a chemical composition of C, 65.14%; H, 5.99%; N, 13.37% for **3a** and C, 65.30%; H, 7.37%; N, 10.40% for **4a**. These values are in good agreement with those of the pure compound **3a** and the corresponding sodium salt of **4a**, respectively. (Calcd for $C_{17}H_{19}N_3O_3$ of **3a**: C, 65.16%; H, 6.11%, N, 13.41%. Calcd for $C_{22}H_{28}N_3 NaO_3$ of **4a**: C, 65.17%; H, 6.96%; N, 10.36%.)

C. FT-IR Analysis. FT-IR measurements were carried out to elucidate the molecular structures of self-organized azopyridine carboxylic acids deposited from alkaline aqueous solutions. The results are shown in Figure 4. Leaflet crystals formed from **3a** (Figure 4a) and fibrous materials made from **3b** (Figure 4b) and **4b** (Figure 4d) exhibited the same bands ascribed to $\nu_{C=O}$, ν_{OH} , and the Fermi resonance, at ca. 1707, 2500, and 1930 cm^{-1} , as those observed for the corresponding

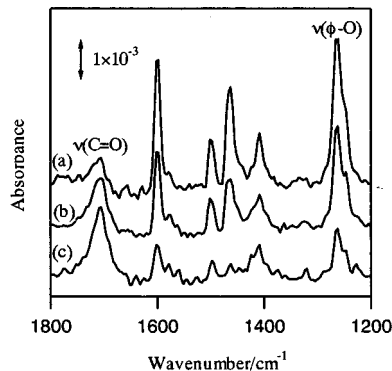


Figure 5. Polarized FT-IR spectra of a microfiber self-organized from **4b** at (a) 0° , (b) 45° and (c) 90° angles between the polarization plane of the probe light and the long axis of the fiber.

pure compounds recrystallized from organic solvents. This indicates the formation of consecutive intermolecular hydrogen bonds in a head-to-tail manner between the pyridyl and carboxyl groups, leading to the self-organization of a pseudopolymer structure by a single-component molecule, as depicted in Figure 1. In contrast, FT-IR spectra of the leaflet crystals formed from an alkaline solution of **4a** (Figure 4c) appeared $\nu_{as,COO^-} = 1554$ cm^{-1} , ascribable to the sodium salt, as supported by the elemental analysis. These results indicate that the fibrous materials of **3b** and **4b** and the leaflet crystals of **3a** are comprised of pseudopolymer structures as a result of hydrogen bond formation between the pyridyl and carboxyl groups in a head-to-tail manner, while the leaflet crystals of **4a** consist of the corresponding sodium salt.

Polarized FT-IR microscopy measurements were performed to obtain further information about the molecular orientations in a microfiber of **4b**. As shown in Figure 5, FT-IR spectra displayed a marked dependence of the absorption band intensity on the angle (θ) made by the long axis of the fiber and the polarization plane of probing light. The maximum for $\nu_{\phi-O}$ and the minimum for $\nu_{C=O}$ appear at $\theta = 0^\circ$, respectively. As presented in Figure 1, the transition moment of the band for $\nu_{\phi-O}$ lies in parallel with the long molecular axis of **4b**, while the $\nu_{C=O}$ band has the transition moment perpendicular to the molecular axis on average. These results indicate decisively that the molecular long axis of the azopyridine carboxylic acid **4b** is aligned parallel to the fiber axis.

D. Powder X-ray Diffraction Analysis. Powder X-ray diffraction (XRD) measurements were carried out to investigate the molecular structures of the resulting self-organized materials. Figure 6a,b shows the XRD patterns observed for fibrous materials of **3b** and for leaflet crystals of **3a**, respectively. Lattice spacings d calculated according to the Bragg equation are also presented in Figure 6. A prominent feature of XRD patterns of the fibrous materials is that the broad peak appears in the region of $2\theta > 20^\circ$ ($d < 0.44$ nm) for the fibrous materials of **3b** with a propyl side-chain substituent as compared to the case for the leaflet crystals of **3a** without the substituent. Analogous diffraction patterns were obtained for the fibrous assemblages of **4b** and leaflet crystals of **4a**. These results support the conclusion that the fibrous materials formed from **3b** and **4b** are not made of crystals and that the pseudopolymer structures are formed as a result of the consecutive formation of intermolecular hydrogen bonds of the azopyridine carboxylic acids in a uniaxial manner, presumably because of the reduction of lateral ordering among pseudopolymer chains. It is obvious that the propyl substituent plays a critical role in the suppression of $\pi-\pi$

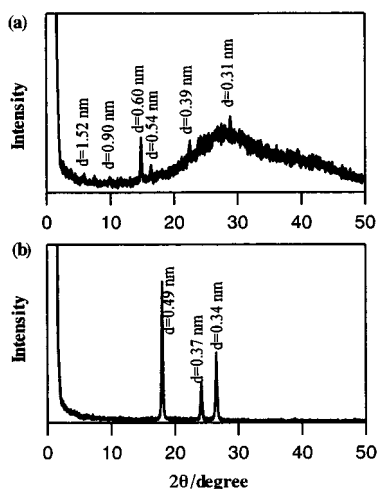


Figure 6. Powder X-ray diffraction patterns of microfibers of (a) **3b** and (b) leaflet crystals of **3a** in a wet state.

stacking among aromatic azopyridine moieties in the self-organized fibrous materials.

Photoinduced Morphological Changes of Self-Organized Materials. It is of great interest to investigate the influence of photoirradiation on the self-organization behavior of the amphoteric azopyridine carboxylic acids, because *E*–*Z* photoisomerization of aromatic azo-compounds generally brings about the transformation of their chemical structure from the rodlike *E*-isomer to the bent *Z*-isomer. The amphoteric azopyridine carboxylic acid **4b**, dissolved in an aqueous NaOH solution, exhibits an absorption maximum centered at 364 nm due to the π – π^* transition of the azopyridine moiety. Photoirradiation of the aqueous solution of **4b** with monochromatic 365-nm light caused *E*-to-*Z* photoisomerization of **4b**, displaying a decrease in the absorbance at 364 nm and an increase in the absorbance at 440 nm due to the n – π^* transition in addition to the appearance of an isobestic point at 425 nm. When the solution was illuminated with light of >350 nm, the proportion of *Z*-isomer at the photostationary state was reduced because of the simultaneous n – π^* excitation. *E*-to-*Z* photoisomerizability on irradiation with 365- and >350 -nm light was estimated to be 38 and 18%, respectively.²⁴ The *Z*-to-*E* thermal reversion was completed within a few hours in the dark at room temperature. On the other hand, no spectral change due to *E*–*Z* photoisomerization occurred, even when **4b** dissolved in an acidic solvent like acetic acid was exposed to 365-nm light. These results are in agreement with previous reports on the photoisomerization behavior of phenylazopyridines and azobis(pyridine)s,²⁵ indicating that either protonated or alkylated pyridinium moiety as a strong electron-withdrawing group markedly destabilizes *Z*-isomers due to their electronic structure, similar to a push–pull type of azobenzenes.

To reveal the effect of the coexistence of *Z*-isomer on the formation of the microfibers, aqueous alkaline solutions of **4b** were exposed to light of 365 or >350 nm throughout the deposition of self-organized materials, since the *Z*-isomer of **4b** is reversed to the *E*-isomer within a few hours. When a 0.2 mmol dm^{−3} aqueous solution (0.7 mL) of **4b** containing 20 mmol dm^{−3} NaOH was left to stand for 13–15 h under irradiation with 365-nm light, unique assemblages were formed,

(24) *E*-to-*Z* photoisomerizability was defined as $(A_0 - A)/A_0$, where A_0 and A represent the absorbance at 364 nm (absorption maxima) before and after photoirradiation, respectively.

(25) (a) Brown, E. V.; Granneman, G. R. *J. Am. Chem. Soc.* **1975**, *97*, 621. (b) Nakagawa, M.; Rikukawa, M.; Watanabe, M.; Sanui, K.; Ogata, N. *Bull. Chem. Soc. Jpn.* **1997**, *70*, 737.

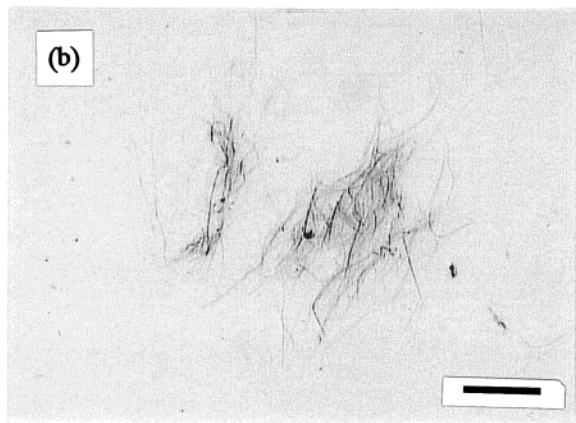
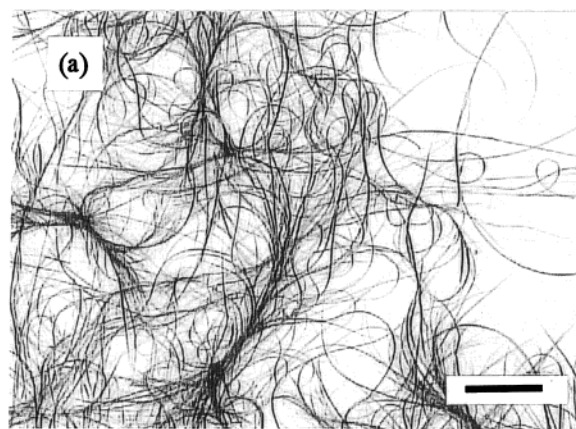


Figure 7. Optical microscopy images of molecular assemblages formed from **4b** (a) in the dark, (b) under irradiation with light at >350 nm, and (c) with UV light at 365 nm, respectively (scale bar: 100 μ m).

with needlelike fibers radiating from each single point, as shown in Figure 7c. The morphology of the assemblages is quite different from that deposited from an aqueous alkaline *E*-isomer of **4b** in the dark (Figure 7a). Careful comparison of part a of Figure 7 with part c indicates that the growth of needlelike materials along with the propagation direction of the microfibers is suppressed under the photoirradiation. The illumination with >350 -nm light to give a photostationary state of a lower level of *Z*-isomer caused intermediate morphological features of fibrous materials, as shown in Figure 7b. Consequently, it may be concluded that morphological features of the molecular assemblages are controllable by light.

Discussion

The amphoteric azopyridine carboxylic acids self-organize into macroscopically well-defined molecular assemblages due

to cooperative intermolecular interactions despite the simplicity of their chemical structure. It is reasonable to conclude that the formation of the molecular assemblages is driven by intermolecular interactions, including the head-to-tail hydrogen bonding between the carboxyl and pyridyl groups, the π - π stacking and the dipole-dipole interactions among the aromatic chromophores, and hydrophobic interactions among the spacer chains, as depicted in Figure 1. Due to the involvement of pyridyl, carboxyl, and azo groups in the molecules, the azopyridine carboxylic acids are sensitive to external stimuli such as heat, pH alteration, and light, which accordingly influence molecular assembling processes decisively as follows. Concerning the effect of heat treatment, supramolecular structures exhibiting pseudopolymer chains formed by consecutive hydrogen bonds in a head-to-tail manner undergo reversible depolymerization to and polymerization from small molecular species such as a monomer and/or a dimer of the azopyridine carboxylic acid upon heating. The azopyridine carboxylic acids dissolve in an aqueous alkaline solution as carboxylate anions, which are neutralized gradually by atmospheric carbon dioxide to give fibrous materials as supramolecular assemblages when a propyl substituent is introduced at the aromatic ring. Photoirradiation of the alkaline solution influences the self-organization process to deform the morphology of the fibrous materials. A detailed discussion on the effect of these factors on molecular assemblages of the azopyridine carboxylic acids is given below.

Organized Structure Affected by Heat. As revealed by FT-IR measurements presented in Figure 2, heating of **3a** at temperatures above the melting point (173 °C) results in the disappearance of the absorption bands at 1707, 1930, and 2500 cm^{-1} due to the formation of consecutive hydrogen bonds between the carboxyl and pyridyl groups, leading to the appearance of the band at ca. 3000 cm^{-1} ascribable to carboxylic acid dimers (Figure 2c). Upon cooling below the melting point, the thermally generated dimeric species are transformed again to give the head-to-tail coupled and hydrogen-bonded pseudopolymer structure. Closely related works were reported previously on binary systems consisting of pairs of pyridine and carboxylic acid derivatives to give supramolecular liquid crystals and liquid crystalline polymers.^{11,12} The self-organized liquid crystalline materials formed through hydrogen bonds in this way display the cleavage of the hydrogen bonds over a phase transition temperature between a mesophase and an isotropic phase. To the authors' knowledge, the present observation is the first example of the thermoreversible structuring of pseudopolymers starting from single compounds. The consecutive formation of hydrogen bonds in a head-to-tail manner to give thermodynamically stable pseudopolymer structures plays an essential role in the self-organization of azopyridine carboxylic acids.

Self-Organization Affected by pH Change. The amphoteric azopyridine carboxylic acids are soluble in basic and acidic organic solvents such as pyridine and acetic acid. Such amphoteric compounds, except for **4a**, are readily dissolved also in alkaline aqueous solutions, whereas they show poor solubility in a neutral aqueous solution. This makes it possible to control the deposition of the azopyridine carboxylic acids from alkaline solutions by gradual neutralization to form molecular assemblages through the formation of consecutive hydrogen bonds. In fact, the azopyridine carboxylic acids (**3a**, **3b**, and **4b**), dissolved in alkaline aqueous solutions as carboxylate anions, were deposited by aging under atmospheric conditions for neutralization with atmospheric carbon dioxide to give molecular assemblages containing no alkaline metal salt. The morphology of the molecular assemblages was remarkably dependent on the

chemical structure of the azopyridine carboxylic acids. **3b** and **4b** with a propyl side chain gave fibrous materials exhibiting less crystallinity, while leaflet crystals were obtained from **3a** and **4a**, both of which bear no substituent, as shown in Figure 3a-d.

It is worth noting that the fibrous materials and the leaflet crystals of **4a** had quite different chemical compositions. The FT-IR measurements and elemental analyses indicate clearly that the fibrous materials of **3b** and **4b** and the leaflet crystals of **3a** consist of pseudopolymers of azopyridine carboxylic acids as a result of head-to-tail coupled hydrogen bonding, whereas the leaflet crystals made from **4a** consist of sodium salts of azopyridine carboxylate. For the self-organization process of fibrous materials, it is assumed that the azopyridine carboxylate anions in an alkaline solution are neutralized gradually by atmospheric carbon dioxide to form the intermolecular hydrogen bonds. Indeed, the deposition of molecular assemblages took place at pH 6 for **2b**, pH 9 for **3b**, and pH 10 for **4b**. Imae⁸ and Shimizu^{10b} reported analogous results for the unusually facile protonation of carboxylic acid derivatives when the length of their methylene chains was increased. In addition, Shimizu et al. reported that the neutralization of an alkaline aqueous solution containing a bolaamphiphile with two carboxyl groups by atmospheric carbon dioxide leads to the formation of hydrogen-bonded microtubes.¹⁰ These facts are consistent with our observation, indicating that precursor aggregates of the azopyridine carboxylate anions were formed probably due to hydrophobic interactions among the methylene spacers. These precursors presumably act as nuclei, leading to the one-dimensional growth of the head-to-tail coupled hydrogen bonds as a consequence of neutralization by carbon dioxide in the air.

The next process involves the self-assemblages of the linear pseudopolymers into submicron fibers with a diameter of ca. 350 nm for **3b** and of ca. 200 nm for **4b** as shown in Figure 3e,f. It is anticipated that the formation of the hydrogen bonds results in the enlargement of dipole-dipole interactions among the pseudopolymer chains, which is essential in the self-organization of the pseudopolymer chains in the lateral directions to give the fibrous materials. This anticipation is supported by the polarized FT-IR microscopy measurements, which reveal that the maximum intensity of $\nu_{\phi-\text{O}}$ as the probe band for the molecular axis lies at the direction parallel to the fiber axis (Figure 5).

The absence of the propyl substituent in the azopyridine carboxylic acids (**3a** and **4a**) causes crystallization to give leaflets as a result of strong π - π stacking forces and dipole-dipole interactions among the azopyridine chromophores. In other words, the propyl substituent plays a crucial role in reducing the molecular interactions in the lateral directions to suppress the crystallization. The occurrence of the strong π - π stacking in leaflet crystals of **3a** and **4a** was confirmed by powder X-ray diffraction measurements, as shown in Figure 6, exhibiting clear peaks in the wide-angle region ($2\theta > 22^\circ$, $d < 0.4$ nm). It should be mentioned here that crystalline leaflets of **4a** are composed of the corresponding sodium salt, whereas the crystalline leaflets of **3a** obtained from an alkaline solution are identical with the pure **3a** recrystallized from ethanol. The marked difference stems from the lower solubility of **4a** in an alkaline aqueous solution due to the strong molecular interactions, including the π - π stacking of the aromatic rings, the dipole-dipole interactions, and hydrophobic interactions among the decamethylene spacer chains. Because THF was added to an alkaline aqueous solution to obtain a homogeneous solution of **4a**, the evaporation of THF occurred more rapidly when

compared with the neutralization with atmospheric carbon dioxide, to result in recrystallization of the sodium salt.

Changes in Organization Morphology by Light. Since the moderation of molecular interactions of the azopyridine carboxylic acids in the lateral directions is a key to assembling fibrous materials as supramolecular aggregates, as discussed above, the photoconversion into the *Z*-isomer is an alternative way to modulate the lateral molecular interactions. Three kinds of alkaline aqueous solutions of **4b** with different levels of the photoisomerization were subjected to gradual deposition of insoluble materials. As shown in Figure 7, it was found that the growth of the resulting supramolecular assemblages was hindered efficiently by the increment of *Z*-isomer contents. It should be stressed that the materials deposited under the photoirradiation exhibit XRD patterns identical with those of the fibrous materials made from the *E*-isomer of **4b** in the dark, irrespective of their different morphologies. If we accept, in the foregoing formation process, that fluidlike micelles or bilayers nucleate the growth of the submicrofibers, photoinduced *Z*-isomer should affect the shapes of the nucleating species. This is very likely to be the case, because the molecular structure of azopyridine carboxylate anions composing the nuclear species can be modified by *E*-to-*Z* photoisomerization upon UV light irradiation, and because the photoinduced *Z*-isomer possesses a different basicity in comparison with the *E*-isomer,^{25a} altering the strength and direction of hydrogen bonding. Attention has to be given to the fact that the protonation of the *Z*-isomer of **4b** leads to rapid *Z*-to-*E* thermal reversion in solutions. Since the short lifetime of the photoinduced *Z*-isomer prevents our further studying the nucleation process in detail, another system is under investigation.

Conclusion

Amphoteric azopyridine carboxylic acids display characteristic self-organization behavior due to multiple intermolecular

interactions involving hydrogen bonding, π - π stacking, dipole-dipole interactions, and hydrophobic interactions. Heat treatment of the linear pseudopolymers arising from head-to-tail coupled hydrogen bonding between pyridyl and carboxyl residues caused reversible supramolecular polymerization. The gradual neutralization of alkaline aqueous solutions of the azopyridine carboxylic acids (**3b** and **4b**) with the propyl substituent induced by atmospheric carbon dioxide brought about the self-organization of well-defined submicrofibers. *E*-to-*Z* photoisomerization of **4b** affects morphological features of the fibrous materials such as the length of the fibers and the number of branching points, depending on the level of *Z*-isomer content. That is to say, molecular-level modifications arising from external stimuli including heat, pH, and light are amplified by the self-organization process through cooperative effects of multiple noncovalent intermolecular interactions on their organization morphology at the macroscopic level. We expect that these systems develop further to create progressive molecular assemblages having the desired morphology and functionality on demand.

Acknowledgment. The authors are grateful to Mr. Kimura and Mr. Nakano of Nippon Bio-Rad Laboratories for polarized FT-IR microscope measurements. We are grateful to Professor Takashi Kato of the University of Tokyo and Professor Takahiro Seki of Tokyo Institute of Technology for their helpful discussions.

Supporting Information Available: Experimental section (material, deposition of an azopyridine carboxylic acid from an alkaline solution, physical measurement, and photoirradiation) (PDF). This material is available free of charge via the Internet at <http://pubs.acs.org>.

JA001790F